Typhoon: a vortex-lattice method for assessing dynamic stability characteristics of hydrofoil crafts with foils within proximity of the free-surface

Alec Bagué

Supervisor(s): Prof. dr. ir. J. Degroote, ir. T. Demeester, Prof. dr. ir. E. Lataire

Abstract—**In this paper the implementation of a vortex-lattice method to perform a dynamic stability analysis for hydrofoil crafts is discussed.**

Keywords—**foiling, vortex-lattice method, free-surface, dynamic stability**

I. Introduction

In this paper the implementation of a vortex-lattice method to perform a dynamic stability analysis (DSA) for hydrofoil crafts is discussed. Hydrofoiling is the practice where a normally buoyant vessel is fitted with lifting surfaces below the water surface which generate an upwards force. This lift will then partly or completely replace the buoyant force of the hull. If this force becomes sufficiently large, it will lift the hull out of the water as if the boat were flying. As the hull is lifted from the water, there is an ensuing reduction of the drag as now only the hull's appendages are (partly) submerged. This is a clear advantage as it allows for greater speeds for the same propulsive power. The increase in speed and the radically different way of sailing has however led to new and greater risks: some accidents have already occurred [4]. In the pursuit of making foiling more mainstream, safety is one of the primary concerns.

One way of providing sufficient safety is to examine and improve the stability of hydrofoil boats as this will lead to more predictable behaviour and easier handling, this can be done by performing a DSA. However, in present day designs of hydrofoil crafts, the assessment of the dynamic stability is often lacking whereas in aeroplanes it is common practice. The working principles of a hydrofoil craft are nonetheless very similar to those of an aeroplane, with the exception of the added complexity of the free-surface. This means a lot of existing knowledge on aeroplane theory can be extended to hydrofoil crafts. The DSA is performed by linearizing the dynamic and kinematic equations, and substituting the forces for their first-order Taylor expansions with force derivatives for all the different motion variables. A more profound explanation of the DSA and the linearization of the system can be found in the work by Drela [2]. The DSA especially for hydrofoil crafts is explained in the work by Masuyama [5] or more recently by Bagué et al. [1].

The reason why the assessment of the dynamic stability in hydrofoil crafts is often lacking can be attributed to the lack of widely available and easy-to-use tools such as is the case for aeroplanes. If you were to attempt to perform such a DSA for the design of a hydrofoil craft today, you should turn to CFD packages and would have to run a multitude of costly flow calculations, which is often way past the budget of boat builders, and even then you would have to set up an entire framework yourself. In contrast, for aeroplanes there exists a variety of different potential-flow codes which allows professionals and amateurs alike to perform swift flow calculations and dynamic stability analyses. Some of many examples are AVL by Drela and Youngren [10] written in Fortran or Tornado by Tomas Melin [6] implemented in Matlab. These programs allow you to define a certain aeroplane geometry and perform various flow calculations or a DSA for this geometry. Both these programs are available under the GNU General Public License.

This paper discusses the implementation of such a code specifically for performing flow calculations and performing the DSA of hydrofoil crafts. This code should be an easy-to-use tool which can perform simple dynamic stability analyses to compare different designs. After comparing Prandtl's lifting-line method and the vortex-lattice method, it was concluded that the vortex-lattice method was better suited for the problem at hand as it did not need any preexisting knowledge on lift- and drag-coefficients, such as is the case for Prandtl's lifting-line method. The code, which will be named Typhoon, will be implemented in Matlab and will use Tornado as its basis. The choice to use Tornado as a starting point is because it has an existing framework to define a geometry and use a vortex-lattice method to do flow calculations. Typhoon will use and extend this vortex-lattice method by adding an additional boundary condition for the free-surface.

II. Governing equations

In this paper the flow will be assumed to be incompressible and inviscid. We will assume a right-handed axis system o_xyz with the origin on the undisturbed free-surface and the z-axis normal to the free-surface directed upward, as is displayed in Fig. **??**. In what follows the potential flow problem will be discussed. To start, the standard approach to the vortex-lattice method will be discussed in Sec. II-A. This standard approach is often used in the study of aeroplanes, and does not take into account the free-surface, the foil is situated in an infinite fluid. Understanding this mechanism first will make it easier to understand the vortex-lattice method which does include the free-surface effect which will be discussed afterwards in Sec. II-B. The total velocity potential Φ is a superposition of the free-stream potential ϕ_∞, the potential due to presence of the foil ϕ_B, a potential due to the image of the foil mirrored over the undisturbed free-surface ϕ'_B and a wave-making potential ϕ_w:

$$\Phi = \phi_\infty + \phi_B + \phi'_B + \phi_w \tag{1}$$

The velocity field can be found by taking the gradient of this total potential: $\nabla\Phi$. The terms in Eq. 1 can be grouped in two categories. The first two terms comprise the principal flow and are a part of the standard approach of the vortex-lattice method, they represent the flow around the foil in an infinite fluid. The two latter terms contain the disturbance flow due to interaction between the foil and the free-surface. The presence of the mirror image of the foil can be intuitively understood as follows: the potential due to the presence of the foil ϕ_B and due to its image ϕ'_B both create a vertical velocity at the free surface which is equal in size but opposite in direction. The vertical velocity due to foil will therefore cancel out at the free-surface and it will therefore remain undisturbed. The wave-making potential ϕ_w is therefore superimposed on an undisturbed free-surface. The free-surface disturbance is assumed to be small, which lets us make use of the linear free-surface boundary condition which will be discussed in Sec. II-B.
Beneath the free-surface, inside the flow region a series of conditions has to be met by the total velocity potential:

$$\nabla^2\Phi = 0 \tag{2}$$

$$|\nabla\Phi| < \infty \text{ at TE of the foil} \tag{3}$$

$$\Phi \to xU \text{ for } x \to -\infty \tag{4}$$

$$\Phi \to xU \text{ for } z \to -\infty \tag{5}$$

These conditions agree respectively with the Laplace equation which expresses the incompressibility, the Kutta condition which states that there is has to be a stagnation point at the sharp trailing edge of the foil, the radiation condition which states that the waves cannot travel upstream of the foil which means that the total velocity potential there simply reduces to the free-stream potential $\phi_\infty = xU$ and lastly the depth condition.

A. *Vortex-lattice method*

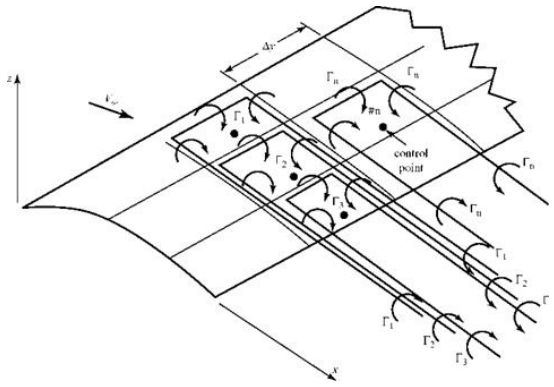

Fig. 1. A representation of the discretization of a foil and of the horseshoe vortices.

In this paragraph the method to calculate the principal flow problem will be discussed, it results in the flow around the foil in an infinite fluid. As mentioned in Sec. I, Typhoon will make use of a vortex-lattice method to calculate the lift and drag of the foils. The basic idea behind the vortex-lattice method is that every wing/foil gets discretized into different panels. This discretization happens in both the span- and chordwise direction. To every panel, a horseshoe vortex with a constant circulation strength Γ_i is assigned. Every vortex is comprised of three straight segments: two trailing legs extending to infinity and one shorter leg connecting the two other legs completing the "horseshoe". This connecting segment is located at the one-quarter chordwise position of the panel. An overview of this can be found in Fig. 1.

An infinitesimal vortex filament results in a flow around it which can be obtained from the law of Biot-Savart as shown in Eq.6. In this equation Γ_i is the circulation strength of that particular vortex, $\overrightarrow{r}(x,y,z)$ is the position vector of the point where the velocity contribution calculated, $\overrightarrow{dl}'(\xi,\eta,\zeta)$ is an infinitesimal segment of the vortex (a vortex filament) and $\overrightarrow{r}'(\xi,\eta,\zeta)$ is the position vector of this segment. The variables (ξ,η,ζ) and (x,y,z) are written here but will be omitted in future equations for simplicity. The coordinates (x,y,z) always relate to a point in space where the flow is to be calculated, whereas the coordinates (ξ,η,ζ) are related to the position on the horseshoe vortices which affect the afore mentioned point. Fig. 2 gives a nice overview of the different variables.

$$d\overrightarrow{V}'(\overrightarrow{r}) = \frac{\Gamma_i}{4\pi}\frac{\overrightarrow{dl_i}'(\xi,\eta,\zeta)\times(\overrightarrow{r}(x,y,z)-\overrightarrow{r_i}'(\xi,\eta,\zeta))}{|\overrightarrow{r}(x,y,z)-\overrightarrow{r_i}'(\xi,\eta,\zeta)|^3} \tag{6}$$

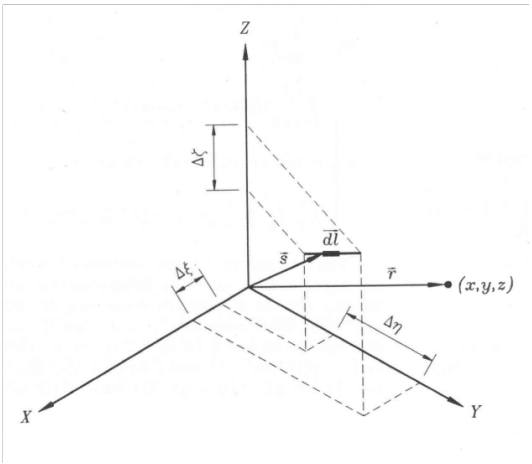

Fig. 2. The representation of a general vortex filament [8]

The contribution $\overrightarrow{V}'$ of a complete horseshoe vortex to the total velocity field can be found by solving the Biot-Savart line integral as shown in Eq. 7. The integral runs over the entire horseshoe vortex, which consist of three parts: the two trailing vortices and the connecting segment.

$$\overrightarrow{V}'(\overrightarrow{r}) = \frac{\Gamma_i}{4\pi}\int\frac{\overrightarrow{dl_i}'\times(\overrightarrow{r}-\overrightarrow{r_i}')}{|\overrightarrow{r}-\overrightarrow{r_i}'|^3} \tag{7}$$

When superimposing the free-stream contribution and all the contributions of every horseshoe vortex the entire flow field can

be constructed. When there are N panels this results in the following equation:

$$\begin{aligned}\overrightarrow{V}(\overrightarrow{r}) &= \sum_{i=1}^{N} \frac{\Gamma_i}{4\pi} \int \frac{\overrightarrow{dl_i}' \times (\overrightarrow{r} - \overrightarrow{r_i}')}{|\overrightarrow{r} - \overrightarrow{r_i}'|^3} - (\overrightarrow{U} + \overrightarrow{\Omega} \times \overrightarrow{r}) \\ &= \sum_{i=1}^{N} \Gamma_i \hat{V}_i(\overrightarrow{r}) - (\overrightarrow{U} + \overrightarrow{\Omega} \times \overrightarrow{r})\end{aligned} \tag{8}$$

The variable $\hat{V}_i(r)$ is a kernel function and expresses the influence the i'th horseshoe vortex has on a point r in space. From the equations above it is clear that this function, which is nothing more than the Biot-Savart integral, is only affected by the orientation of the horseshoe vortex and the relative distance between this vortex and the point r. This means this kernel function is not affected by the state of a craft but is property of the geometry of the craft.

There however still remains the question of how the vortex strengths or circulations Γ_i will be calculated as these are not only affected by the geometry but also by the state of the foil (speed, AoA, ...). Therefore an additional boundary condition will have to be met. This Dirichlet boundary condition states that there can be no flow in the normal direction to the camber surface of the foil. Note that we impose this Dirichlet boundary condition on the camber surface instead of the foil surface, this nuance means that thickness will not bet taken into account. This is because in the typical operating range buoyancy becomes negligible. The boundary condition will be imposed in the so-called collocation point (or control point) which is situated at the three-quarter chordwise position on each panel. Every collocation point (except that one on the most rearwards panel) will be located halfway between two subsequent horseshoe vortices. This Dirichlet boundary condition can be expressed as follows with $\overrightarrow{r}_j^c$ the location of the j'th collocation point:

$$\begin{aligned}\frac{\partial \phi}{\partial n} &= \overrightarrow{V}(\overrightarrow{r}_j^c) \cdot \overrightarrow{n}_j = 0 \\ &\leftrightarrow (\sum_{i=1}^{N} \Gamma_i \hat{V}_i(\overrightarrow{r}_j^c) - (\overrightarrow{U} + \overrightarrow{\Omega} \times \overrightarrow{r}_j^c)) \cdot \overrightarrow{n}_j = 0 \\ &\leftrightarrow (\sum_{i=1}^{N} \Gamma_i (\hat{V}_i(\overrightarrow{r}_j^c) + \hat{V}_i, w(\overrightarrow{r}_j^c)) - (\overrightarrow{U} + \overrightarrow{\Omega} \times \overrightarrow{r}_j^c)) \cdot \overrightarrow{n}_j = 0\end{aligned} \tag{9}$$

All the different contributions can be superimposed to find the total speed at the collocation point. In this case the total velocity is the superposition of the contribution of every vortex, the free-stream velocity and the rotation induced velocities.

In the context of a computational environment like Matlab it makes more sense to to be expressing everything in a vectorized format. In a case with N panels, the flow trough the collocation point for every panel is affected by the $N-1$ other panels and by the panel itself. This means that the matrix notation of the kernel function $[\hat{V}]$ becomes an $N \times N \times 3$ matrix, in which the first index represents the number of the collocation point, the second index represents the number of the affecting horseshoe vortex and the last index is the dimension. E.g. element $(15, 2, 3)$ is how the 15'th panel is affected by the second panel in the z-direction. If now every element of this kernel matrix gets multiplied with the normal of the affected panel, as in Eq. 10, the aerodynamic influence coefficient (AIC) matrix is found or in our case the hydrodynamic influence coefficient (HIC) matrix $[H]$. This HIC matrix is a $N \times N$ matrix. For the example above, we would have to multiply the vector at position $(15, 2, :)$ with the normal vector of the 15'th panel to express how the 15'th panel is affected by the 2nd panel.

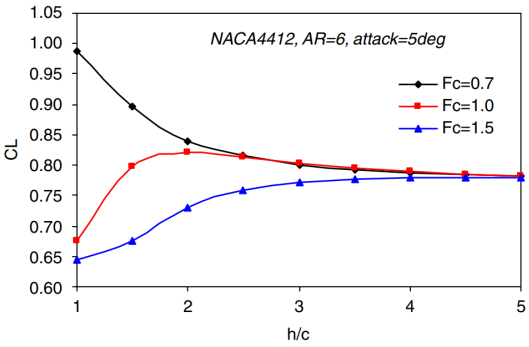

Fig. 3. Results by Xie and Vassalos[9]

$$H_{ij} = \hat{V}_j(\overrightarrow{r}_i^c) \cdot \overrightarrow{n}_i \tag{10}$$

B. Free-surface

The procedure above allows us to calculate the principal flow in the case of the foil being subject to a steady free-stream velocity U. The resulting lift coefficient is therefor independent of both the velocity and the proximity to the free surface. The lift coefficient as a function of submergence and speed has been studied by, amongst others, Faltinsen and Semenov [3] and by Xie and Vassalos [9]. Fig. 3 shows the lift coefficient as a function of the dimensionless submergence (submergence divided by the chord length: h/c) and with the Froude number as a parameter (Froude number based on the chord Fr_c). At low submergence ($h/c < 3$) the speed dependency of the lift coefficient becomes apparent, while for higher submergence ($h/ > 4$) the speed dependency disappears.

Fig. 4 shows a similar figure, but now with the Froude number Fr_c as a function variable and the submergence h/c as a parameter. The lift coefficient is now expressed as a ratio to the lift coefficient in an infinite fluid. From the three different curves, it is clear that with lower submergence the behaviour deviates more from the behaviour in an infinite fluid. Even at high submergence ($h/c = 5$) there is a deviation from the infinite fluid behaviour at high Froude numbers ($Fr >> 1$).

The presence of the free-surface will be modelled by adding an additional boundary condition. This boundary condition is the linearized free-surface boundary condition which is constituted of the kinematic boundary condition (KBC) and the dynamic boundary condition (DBC). The KBC states that the free-surface is a streamline and that particles on the free surface follow the vertical motion of the free-surface. The DBC states that the pressure on the free-surface remains invariant. The elevation of the free surface is expressed as $z = \zeta(x, y)$. The total

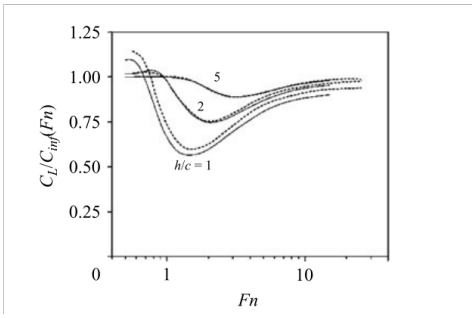

Fig. 4. Results by Faltinsen[3]

potential can be divided in the free-stream component and the disturbance component due to the foil such as is displayed in Ea. 11, which allows us to write the corresponding velocities:

$$\Phi = U \cdot x + \phi \tag{11}$$

$$\Leftrightarrow \begin{cases} u = U + \frac{\partial \phi}{\partial x} \\ w = \frac{\partial \phi}{\partial z} \end{cases} \tag{12}$$

B.1 Kinematic boundary condition

The KBC states that the fluid velocity at the surface is tangential to the free-surface, which can be expressed as follows:

$$\begin{aligned} \frac{\partial \zeta}{\partial x} &= \frac{w}{u} \qquad \text{at } z = \zeta \\ &= \frac{\frac{\partial \phi}{\partial z}}{(U + \frac{\partial \phi}{\partial x})} \\ &= \frac{1}{U}\frac{\partial \phi}{\partial z}(\frac{1}{1 + \frac{1}{U}\frac{\partial \phi}{\partial x}}) \end{aligned} \tag{13}$$

The last expression in Eq. 13 can be approximated using a first order Taylor approximation around 0. The term $\frac{\partial \phi}{\partial x}$ is assumed to be many times smaller than the free-stream velocity U which is why the linear approximation suffices. This is shown in Eq. 14

$$\frac{\partial \zeta}{\partial x} = \frac{\frac{\partial \phi}{\partial z}}{(U + \frac{\partial \phi}{\partial x})} \approx \frac{1}{U}\frac{\partial \phi}{\partial z}(1 - \frac{1}{U}\frac{\partial \phi}{\partial x}) \tag{14}$$

$$\Leftrightarrow \frac{\partial \zeta}{\partial x} = \frac{1}{U}\frac{\partial \phi}{\partial z} \tag{15}$$

Dynamic boundary condition

The DBC states, as expessed earlier, that the dynamic pressure on the free-surface remains unchanged. This can be expressed using Bernouilli's equation where the left hand side is for a point far upstream on the undisturbed free-surface and the right hand side is for a point in the proximity of the foil:

$$\rho\frac{U^2}{2} + p_a = p + \frac{1}{2}\rho[(\frac{\partial \phi}{\partial x})^2 + (\frac{\partial \phi}{\partial y})^2 + (\frac{\partial \phi}{\partial z})^2] + \rho g z \qquad \text{at } z = \zeta \tag{16}$$

Naturally the pressure at the free-surface is that of the atmosphere ($p = p_a$) and the equation reduces to:

$$\Leftrightarrow -\frac{1}{2}\rho U^2 + \frac{1}{2}\rho[(U + \frac{\partial \phi}{\partial x})^2 + (\frac{\partial \phi}{\partial y})^2 + (\frac{\partial \phi}{\partial z})^2] + \rho g \zeta = 0 \tag{17}$$

Neglecting the second order terms of the small terms gives:

$$\begin{aligned} \Leftrightarrow -\frac{1}{2}U^2 + \frac{1}{2}\rho[U^2 + 2U\frac{\partial \phi}{\partial x}] &= -g\zeta \\ \Leftrightarrow U\frac{\partial \phi}{\partial x} &= -g\zeta \\ \Leftrightarrow \frac{\partial^2 \phi}{\partial x^2} &= -\frac{g}{U}\frac{\partial \zeta}{\partial x} \end{aligned} \tag{18}$$

Linearized free-surface boundary condition

Combing Eq. 15 & 18 then leads to the following equation, which is the linearized free-surface boundary condition:

$$\frac{\partial^2 \phi}{\partial x^2} + \frac{g}{U^2}\frac{\partial \phi}{\partial y} = \frac{\partial^2 \phi}{\partial x^2} + \kappa_0 \frac{\partial \phi}{\partial y} = 0 \qquad \text{at } z = \zeta \approx 0 \tag{19}$$

This boundary condition has to be added to the list of Eq. 2-5 as a fifth boundary condition. This boundary condition, which was elaborated in the paragraphs above starts from the assumption that the free-surface is previously undisturbed. It was explained above in Eq. 1 that the flow is comprised of two categories, the principal flow due to the free-stream and the foil in an infinite fluid and the disturbance flow due to the interaction of the principal flow with the free-surface. The principal flow however already imposes vertical pressure and velocity gradients on the free-surface, meaning that there would be two potential components contributing to the free-surface disturbances. This difficulty is resolved by adding the image of the foil mirrored over the undisturbed free-surface. This ensures that all the vertical contributions at the free-surface are exactly zero: $w_{z=0} = 0$. The wave-making potential consequently acts upon an undisturbed free-surface.

Plugging the total potential of Eq. 1 into Eq. 19 allows to determine the wave-making potential, the resulting equation is displayed in Eq. 21. The free-stream potential disappears from the equation since it has no second derivative to x nor a first derivative to z. The wave-making potential remains in the equation both as a derivative to x as a derivative to z. The potential due to the foil ϕ_B and its image ϕ'_B do have a second derivative to x at the free surface but have no first derivative to z due to the nature of their definition. The second derivative to x of the potential due to the foil and its image, can also be written as the first derivative to x of the vortex induced x-velocity at the free-surface du_0 which can be calculated using Eq. 6. This is explained more in detail in Thiart's work [8] but the result is given here:

$$\begin{aligned} du_0 &= du_{B,z=0} + du'_{B,z=0} \\ &= -\frac{\Gamma}{2\pi}\frac{\zeta d\eta + (y - \eta)d\zeta}{\{(x - \xi)^2 + (y - \eta)^2 + \zeta^2\}^{3/2}} \end{aligned} \tag{20}$$

$$\left[\frac{\partial^2}{\partial x^2}(d\phi_w) + \kappa_0 \frac{\partial}{\partial z}(d\phi_w)\right]_{z=0} = -\frac{\partial}{\partial x}(du_0) \tag{21}$$

For the left hand side a useful solution of the Laplace equation which also satisfies the depth conditions is [7]

$$d\phi_w = \int_{-\pi}^{\pi}\int_0^{\infty} C(\kappa,\nu)exp[\kappa(z+i\omega)]d\kappa d\nu \tag{22}$$

with $\omega = (x-\xi)cos(\nu) + (y-\eta)sin(\nu)$ and $C(\kappa,\nu)$ some function. Substituting Eq. 20 and Eq. 22 in Eq. 21 allows us to find an expression for $C(\kappa,\nu)$. Further elaborating this results in (the first term has to be added to account for the upstream radiation condition, as it cancels out the waves travelling upstream) [8]:

$$\begin{aligned} d\phi_w =& \frac{\Gamma}{2\pi} Re\left[\int_{-\pi/2}^{\pi/2} (tan(\nu)d\zeta - isec(\nu)d\eta)\right. \\ &\left(-i\kappa_\nu exp[\kappa_\nu(z+\zeta)+i\kappa_\nu\omega]\right. \\ &\left.\left. +\frac{1}{\pi}\int_0^{\infty}\frac{\kappa}{\kappa_\nu-\kappa}exp[\kappa(z+\zeta)+i\kappa\omega]d\kappa\right)d\nu\right] \end{aligned} \tag{23}$$

By integrating this over the entire bound vortex filament we get the entire wave-making potential of this filament. This happens by integrating from (ξ_l,η_l,ζ_l) to (ξ_r,η_r,ζ_r) where both ξ and ζ are replaced by a function of η [8]. Differentiating the resulting expression to x, y and z gives us the components of the wave-making velocity induced by the vortex filament.

$$u_w = -\frac{\Gamma}{2\pi}\int_{-\pi/2}^{\pi/2} \mathrm{Im}\left[\mathrm{f}\{\mathrm{J_r}-\mathrm{J_l}\}\right]\cos(\nu)\mathrm{d}\nu \tag{24}$$

$$v_w = -\frac{\Gamma}{2\pi}\int_{-\pi/2}^{\pi/2} \mathrm{Im}\left[\mathrm{f}\{\mathrm{J_r}-\mathrm{J_l}\}\right]\sin(\nu)\mathrm{d}\nu \tag{25}$$

$$w_w = -\frac{\Gamma}{2\pi}\int_{-\pi/2}^{\pi/2} \mathrm{Re}\left[\mathrm{f}\{\mathrm{J_r}-\mathrm{J_l}\}\right]\mathrm{d}\nu \tag{26}$$

with $J_r = J(\nu,\xi_r,\eta_r,\zeta_r)$ and $J_l = J(\nu,\xi_l,\eta_l,\zeta_l)$ where J stands for:

$$\begin{aligned} J(\nu,\xi,\eta,\zeta) =& -i\kappa_\nu \exp\{\kappa_\nu(z+\zeta)+i\kappa_\nu\omega\} \\ &+\frac{1}{\pi}\int_0^{\infty}\frac{\kappa}{\kappa_\nu-\kappa}\exp\{\kappa(z+\zeta)+i\kappa\omega\}d\kappa \end{aligned} \tag{27}$$

, and with

$$f = f(\nu,\Delta\xi,\Delta\eta,\Delta\zeta) = \frac{\Delta\eta\mathrm{sec}(\nu)+\mathrm{i}\Delta\zeta\mathrm{tan}(\nu)}{\Delta\xi\mathrm{cos}(\nu)+\Delta\eta\mathrm{sin}(\nu)+\mathrm{i}\Delta\zeta} \tag{28}$$

C. Forces and moments

In the determination of the dynamic stability of the hydrofoil craft we are most interested in the forces and moments the different foils generate. The calculation of these forces and moments under different conditions will allow us to calculate the force derivatives by making use of finite differencing. The results of the Sec. II-A & II-B provided the total velocity field and the circulation of every panel. The Kutta-Joukowski theorem allows us then to calculate the force generated by every panel. The Kutta-Joukoski theorem states that the force per unit length F_i' of a two-dimensional foil section depends on the density of the fluid, the speed which the foil section 'sees' and the circulation around that foil section. This formula can then be applied for every panel with its corresponding velocity $\overrightarrow{V}_i$ and circulation Γ_i. To get the force of a panel F_i, the cross product of the Kutta-Joukowski theorem with the length of the connecting vortex has to be taken as in Eq. 29. At first glance the direction of the connecting vortex might seem arbitrary but changing its direction would alter the sign of the circulation strength and therefor result in the same force. The total force and moment can then be calculated according to Eq. 30 & 31.

$$\overrightarrow{F}_i = \rho\Gamma_i\overrightarrow{V}\times\overrightarrow{l}_i \tag{29}$$

$$\overrightarrow{F} = \sum_{i=1}^{N}\overrightarrow{F}_i \tag{30}$$

$$\overrightarrow{M} = \sum_{i=1}^{N}\overrightarrow{F}_i\times\overrightarrow{r}_i \tag{31}$$

III. Computational

Using this vectorized format the following expression for $[\Gamma]$ is found:

$$[\Gamma] = ([\hat{V}]\cdot[n])^{-1}\cdot\overbrace{([U]+[\Omega\times r])\cdot[n]}^{=\text{RHS}}; \tag{32}$$

The matrices in Eq. 32 have the following sizes in the case that there are N panels: $[\Gamma]$ is a $N\times 1$ matrix, $[\hat{V}]$ is a $N\times N\times 3$ matrix and is often denoted as the aerodynamic influence coefficient (AIC) matrix, the matrix is an $[n]$ is a $N\times 3$ matrix and contains the normal for every panel and lastly the complete matrix $[RHS]$ can be found to be a $N\times 1$ matrix.

(33)

References

[1] A. Bagué et al. "Dynamic stability analysis of a hydrofoiling sailing boat using". In: ().

[2] M. Drela. *Flight Vehicle Aerodynamics*. MIT Press, 2014.

[3] Odd M. Faltinsen and Yuriy A. Semenov. "The effect of gravity and cavitation on a hydrofoil near the free surface". In: *Journal of Fluid Mechanics* 597 (2008), pp. 371–394. ISSN: 00221120. DOI: 10.1017/S0022112007009822.

[4] *Franck Cammas airlifted with serious injury*. https://www.yachtingworld.com/news/french-americas-cup-skipper-franck-cammas-badly-injured-after-being-run-over-by-foiling-catamaran-69178. 2019.

[5] Y. Masuyama. "Stability analysis and prediction of performance for a hydrofoil sailing boat. Part 2: dynamic stability analysis". In: *International Shipbuilding Progress* 34.398 (1987), pp. 178–188.

[6] Tomas Melin. *Tornado, a vortex lattice method implemented in Matlab*. URL: http://tornado.redhammer.se/index.php. (accessed: 09.04.2020).

[7] G. D. Thiart. "Vortex lattice method for a straight hydrofoil near a free surface". In: *International Shipbuilding Progress* 44.437 (Jan. 1997), pp. 5–26. ISSN: 0020868X. DOI: 10.3233/ISP-1997-4443701.

[8] G.D. Thiart. "Generalized Vortex Lattice Method for Prediction of Hydrofoil Characteristics". In: *R & D Journal* 7.September 2000 (2001), pp. 35–46.

[9] Nan Xie and Dracos Vassalos. "Performance analysis of 3D hydrofoil under free surface". In: *Ocean Engineering* 34.8-9 (June 2007), pp. 1257–1264. ISSN: 00298018. DOI: 10.1016/j.oceaneng.2006.05.008.

[10] Mark Drela Harold Youngren. *AVL, extended Vortex Lattice Method*. URL: http://web.mit.edu/drela/Public/web/avl/. (accessed: 09.04.2020).